Geologie en Mijnbouw 71: 91–98, 1992.

The April 13, 1992 earthquake of Roermond (The Netherlands); first interpretation of the NARS seismograms

Hanneke Paulssen,[1], Bernard Dost[2] & Torild van Eck[1]
[1] *Dept. of Geophysics, Institute of Earth Sciences, Utrecht University, P.O. Box 80.021, 3508 TA Utrecht, The Netherlands*
[2] *ORFEUS Data Center, Budapestlaan 4, 3584 CD Utrecht, The Netherlands*

Received 29 June 1992; accepted in revised form 10 July 1992

Key words: Peel Boundary Fault, Roer Valley Graben, seismology, waveform modelling

Abstract

The Roermond earthquake of April 13th, 1992, was recorded by stations of the seismological NARS network located in The Netherlands, Germany, and Belgium. The data of this network allowed an accurate determination of epicenter, focal depth, origin time and focal mechanism of the event.

By an arrival time inversion of P-wave onsets, the epicenter and focal depth were located at 51°10.2' N 5°58.3' E and 21 km, respectively. The relatively large focal depth of about 20 km is confirmed by travel time modelling of additional, later arriving, P-wave phases. The average crustal structure beneath the network was implicitly obtained by matching the travel time variations to the different stations.

The earthquake mechanism, i.e. the direction of movement along the fault plane, is inferred by modelling the polarities and amplitudes of the various phases. The NARS data are best fitted by a dip-slip movement along a fault plane with a strike of 124° and a southwesterly dip of 70° or by dip-slip movement along the perpendicular plane with the same strike. The good agreement of the attitude of the first fault plane with that of the Peel Boundary Fault, combined with the fact that the hypocentral location plots on the downward extension of that fault, indicates that a downward movement of the Roer Valley Graben has taken place along the Peel Boundary Fault.

Introduction

In the early morning of April 13, 1992, 3:20 local time, a strong earthquake occurred in The Netherlands in the vicinity of the city of Roermond. It was the strongest earthquake in The Netherlands ever recorded by seismic instrumentation (operational since 1904), and one of the strongest earthquakes in the region known from historical records (Houtgast 1991). It was comparable in size to the earthquake of 1756 near Düren in Germany at a distance of approximately 50 km (Ahorner 1983). The earthquake was strongly felt in large areas of The Netherlands, Belgium, and Germany, and even felt in northeastern France and some parts of England. It caused severe damage and one person died of a heart attack. The earthquake produced an intensity VII on the MSK scale* in the towns of Roermond and Herkenbosch in The Netherlands, and Heinsberg in Germany.

Apart from the permanent seismic observatories

* Intensity VII on the MSK intensity scale can briefly be described as: most people are frightened and run outdoors; in many buildings of good construction slight damage is caused, many poor buildings suffer heavy damage.

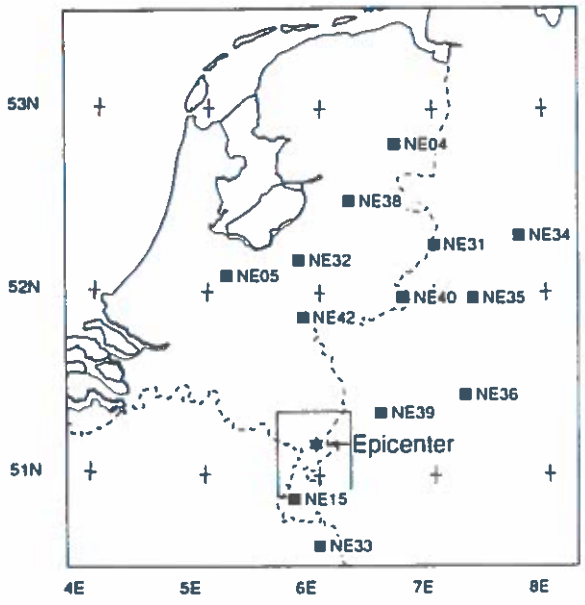

Fig. 1. NARS station configuration. The star indicates the epicenter of the Roermond earthquake. The box indicates the location of the more detailed map of Fig. 4.

that recorded the earthquake worldwide, the Roermond earthquake was also regionally recorded by a mobile network of 3-component broadband digital stations: the Network of Autonomously Recording Seismographs (NARS; Dost 1984; Nolet et al. 1985). NARS, deployed in The Netherlands, Germany, and Belgium since autumn 1989 (Fig. 1), provided a unique suite of seismograms of the Roermond earthquake of which the first interpretation is given here.

The NARS data of the Roermond earthquake: limitations and possibilities

The Roermond earthquake was recorded by 11 of the 13 deployed NARS stations. Covering the epicentral distance range from 50 to 200 km, the data provide the densest digital sampling of the earthquake on these regional distances. Two stations did not record the event, because the recording medium (casette tape) was filled to capacity with previous events. The limited storage capacity of the recorders (2 Mbyte) was already recognized as a severe restriction of the instrumentation, and new dataloggers are therefore currently developed. The most important improvements of the new system are a larger storage capacity (1–2 Gbyte Digital Audio Tape) and a higher dynamic range (130 dB).

Although the NARS instrumentation was not designed to record such a strong local event as the Roermond earthquake, the recordings show their value, for instance in the determination of earthquake location and mechanism. However, one should be cautious with the interpretation of the data. The data show a low-frequency signal on all three components (Fig. 2). For strong local events such a low-frequency signal is observed more often. One possible explanation is a resonance of the helical spring of the seismometer (Aki & Richards 1980). The fact that the low-frequency signal is also observed in the records of the horizontal seismometers which are not equipped with a helical spring, argues against this interpretation and indicates that we may have to look for a cause between the sensors and the recorder.

Before the seismic signal is digitized, it is pre-amplified and (analog) filtered (Dost et al. 1984). The pre-amplifier/filter is designed such that an earthquake of magnitude 7 at an epicentral distance of 2000 km causes saturation of the receiver. Any earthquake of higher magnitude at this epicentral distance will produce an input signal on the pre-amplifier/filter that exceeds its power supply voltage. As a result the signal will be distorted. Similarly, an event of smaller magnitude at a shorter distance may also be distorted by the same mechanism.

In order to estimate the importance of this effect, we calculated the maximum input voltage the pre-amplifier/filter can handle. Since we know the generator constant of the main coil of the seismometer, we are able to calculate the maximum ground velocity, in our case 0.33 mm/s. As a next step we estimated the total gain of each seismograph from the peak-to-peak amplitude of the most recent calibration (Dost 1987) prior to the earthquake and corrected the signal for the instrument response. The result is a record of true ground velocity. From these records one can infer that in most cases the maximum ground velocity is exceeded starting at

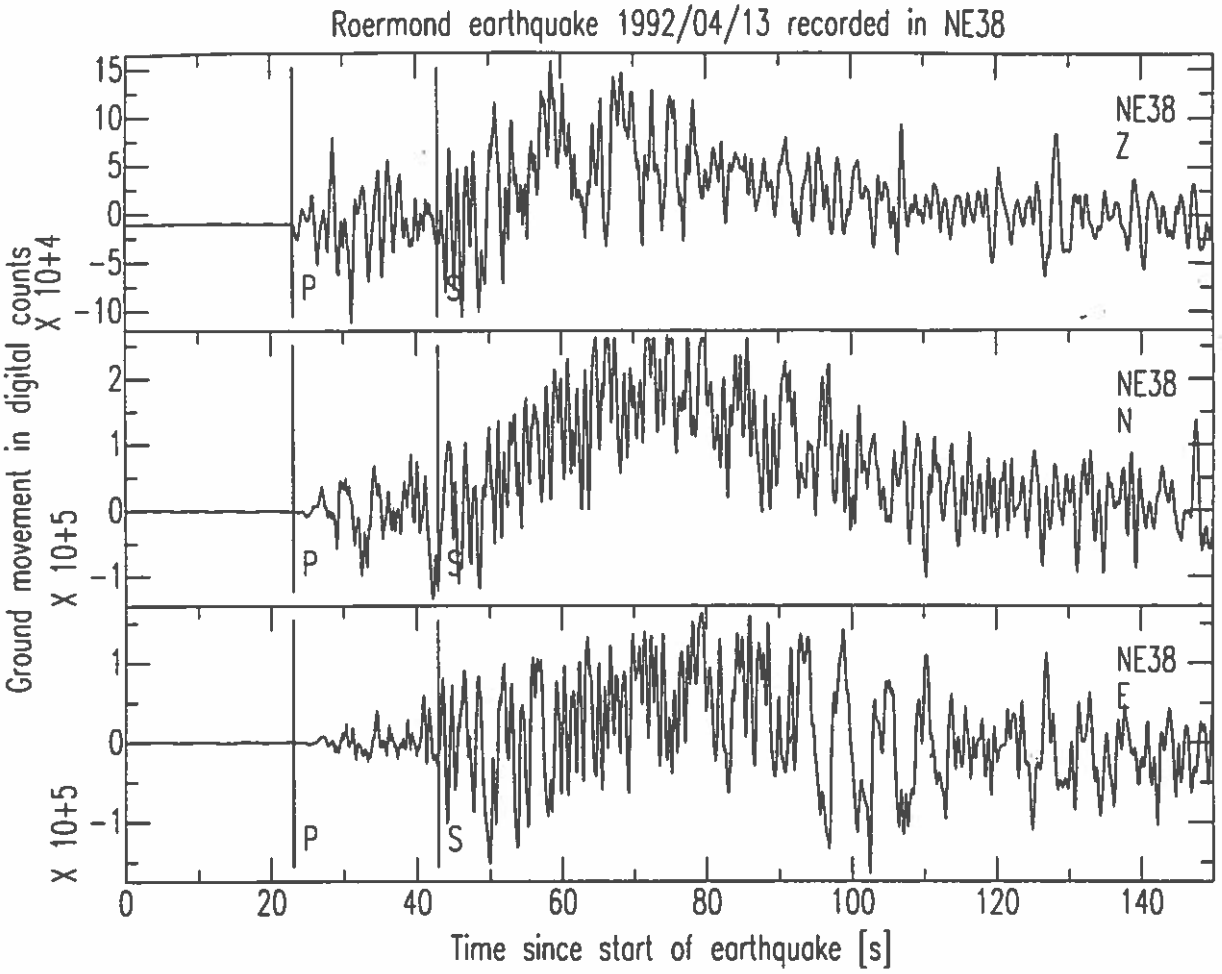

Fig. 2. Vertical, North-South, and East-West recordings of the Roermond earthquake at NE38. P and S mark the first P- and S-wave onsets.

the S-onset, while the P-onset stays within the limits. For nearby stations NE39, and possibly NE33 and NE42, also the P-onset is distorted. The following interpretation therefore concentrates on travel time readings and P-wave amplitudes of the more distant stations.

Epicentral location

An accurate determination of the epicentral location of an earthquake requires arrival time readings from a set of stations that are well distributed with respect to the location of the earthquake. The NARS stations very well fulfill this requirement for the Roermond earthquake (Fig. 1). Moreover, first arrivals on all stations are clear and can be read with an accuracy of ± 0.1 sec. To determine the hypocenter, i.e. epicenter location and focal depth, we need a good model of the crustal velocity structure. We used a layered model of Ahorner & Pelzing (1983; model C, see Fig. 3) with equal wave propagation velocities in each horizontal layer, since our present knowledge of the crustal velocity structure does not justify a more accurate model. The model is based on refraction measurements in the Rhenish Massif and earthquake data from the Roer Valley Graben. This model is probably most

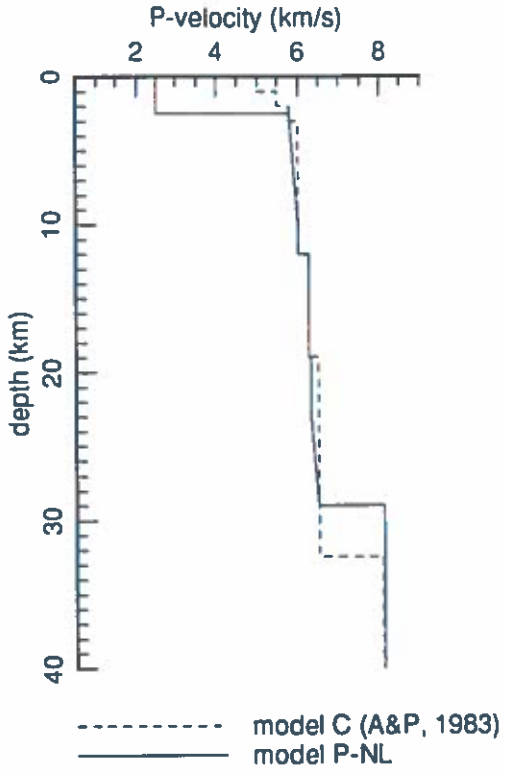

Fig. 3. P-velocity structure used for the determination of the epicentral location (dashed line, model C of Ahorner & Pelzing, 1983), and for modelling the P-wave phases (solid line, model P-NL).

representative of crustal structure beneath the southern part of the NARS network, which is advantageous since the hypocentral location is best constrained by data of the nearby stations.

With the observed NARS P-wave arrival times and the velocity model, the hypocenter is obtained as the solution of an inversion procedure for which we used a modified HYPO71 algorithm (Lee & Lahr 1972; Lienert et al. 1986):

Epicenter:	51° 10.2′ N	5° 58.3′ E
Depth:	21 km	
Origin time:	01:20:03.1 (GMT)	

This epicentral location is in close agreement with the epicenter as obtained by the seismological department of the Royal Netherlands Meteorological Institute (KNMI) using other seismograph stations in The Netherlands, Germany and Belgium (H. Haak, personal communication). The epicenter is located in the Roer Valley Graben (see Fig. 4) at a distance of approximately 7 km from the 'Peelrandbreuk' (Peel Boundary Fault). This suggests that the earthquake at depth may have taken place along this fault. We will examine this hypothesis more closely in the next section.

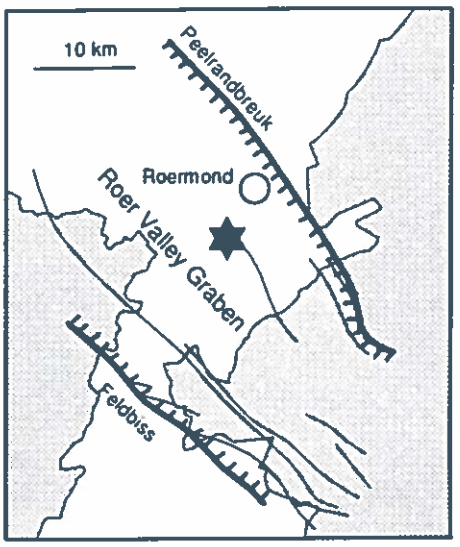

Fig. 4. Epicentral location of the Roermond earthquake (star) in a map of tectonic faults of the area.

It should be noted that the calculated hypocentral depth contains a large uncertainty. An error estimate of 1 km is obtained from mismatches between the observed arrival times with those calculated for the velocity model. However, the uncertainty is probably much larger (in the order of 5 km) due to discrepancies between the true velocity distribution and our model. In spite of the uncertainties, the calculated hypocentral depth remains rather deep, when we realize that – for an earthquake of this size – it indicates the point where rupture is initialized. This point is expected near the bottom of the seismogenic zone (the region of brittle fracture of the crust) which is usually supposed to extend to depths of 12 to 15 km (Scholz 1990). The depth as we find it indicates a deeper extension of the seismogenic zone in this region, as was also suggested by Ahorner (1983) and Ahorner & Pelzing (1983). However, such a conclusion re-

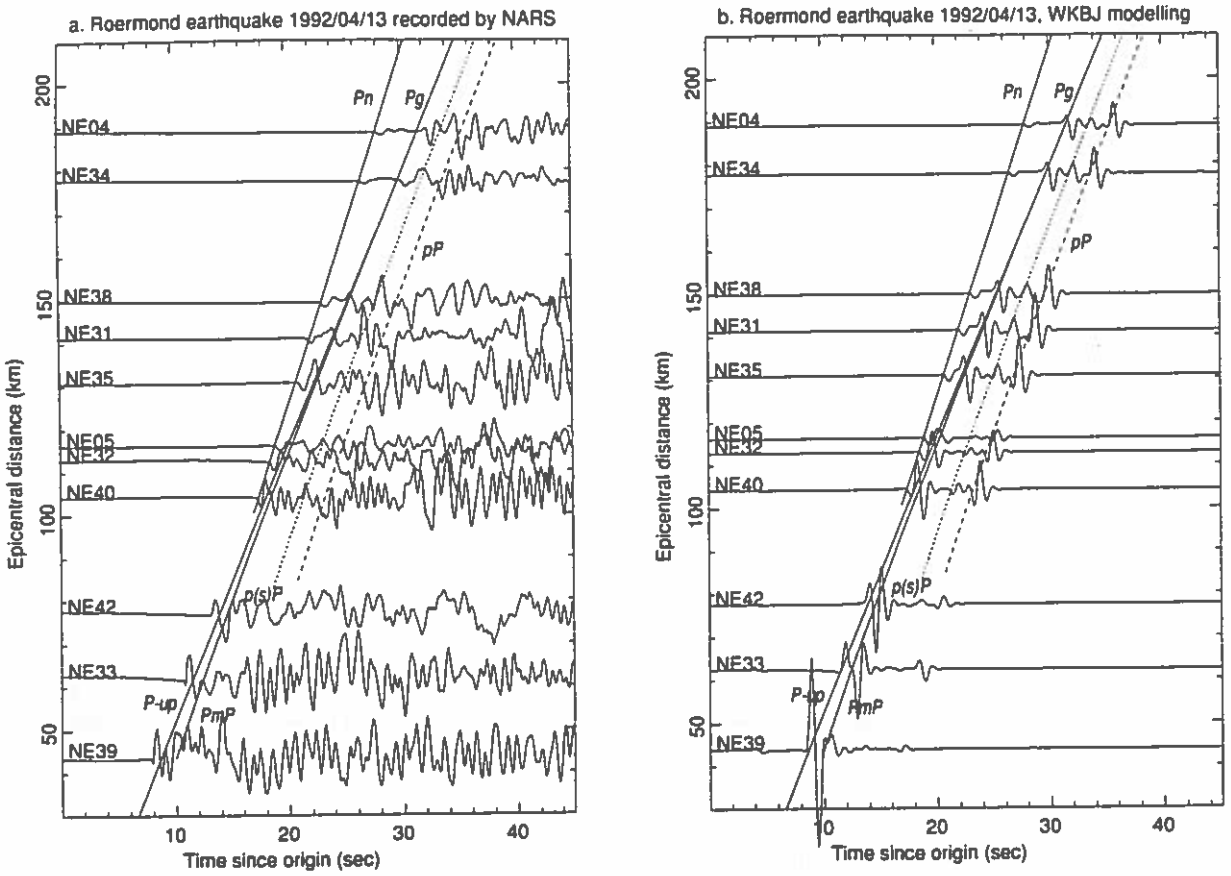

Fig. 5. Comparison of observed and synthetic seismograms of the Roermond earthquake. (a) NARS Vertical component seismograms plotted as function of epicentral distance. (b) Synthetic seismograms obtained by WKBJ modelling. The model parameters are: model P-NL for the velocity structure, a 20 km source depth, and a mechanism of dip-slip movement along a plane with strike 124° and dip 70°. Theoretical travel times of the phases displayed in Fig. 6 are shown in both diagrams. (PmP: Moho-reflected phase).

mains speculative as long as the hypocentral depth is not better constrained.

Modelling the NARS seismograms: earthquake mechanism, depth and velocity structure

The favourable distribution of the NARS stations for the Roermond earthquake further enables an adequate determination of the earthquake (or focal) mechanism, i.e. the direction of movement along the fault plane. The amplitude and polarities of the seismic waves emitted from the source carry the necessary information to reconstruct the movement at the hypocenter. Coventionally, the earthquake mechanism is determined from the polarities of first-arriving P-waves. At the source, the compressions (first motion upward) and dilatations (first motion downward) are separated by two nodal planes. One of them is the fault plane, the other, perpendicular, plane is called the auxiliary plane. A convenient representation of the socalled 'fault plane solution' is an equal area projection of the two nodal planes, where the quadrants of compression are hatched (see Fig. 7).

Because the NARS data contain more information than the sign of first motion, we took a different approach to determine the earthquake mechanism. The initial parts of the seismograms consist of a sequence of seismic phases that travel along different paths in the crust and uppermost mantle. Each phase carries information about the focal

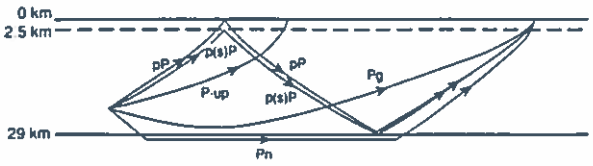

Fig. 6. Schematic representation of the raypaths of the upward travelling P-wave (P-up), the crustal P-wave (Pg), the headwave from the Moho (Pn), the surface-reflected phase (pP), and the phase reflected at the base of the sedimentary layer (p(s)P).

mechanism and the crustal velocity structure. Fig. 5a shows the first parts of the seismograms (vertical component) as a function of epicentral distance (along the vertical axis). Evident from this diagram is the switch in polarity of the first arrival between 80 and 100 km and the change in character of the signal with epicentral distance

We modelled the waveforms of the seismograms and tried to match the polarities of the phases, their relative amplitudes, and their timing. This is not a straightforward procedure, as it requires a correct interpretation of the signal in terms of the different phases. The WKBJ-algorithm (Chapman 1978) was used to compute synthetic seismograms and the data were modelled by trial and error. We were able to identify the most prominent phases, and to model their timing, amplitude and polarity. Figure 5b shows the final synthetic seismograms with an indication of the travel times of the various phases. The raypaths of these phases are schematically presented in Fig. 6. The travel time curves of the phases are also shown in Fig. 5a to facilitate the comparison between data and synthetics.

The signs and amplitudes of the first and later arrivals were adequately modelled by a focal mechanism corresponding to a pure dip-slip movement along a plane with a strike of 124° and a dip of 70° to the southwest, or a dip-slip movement along its perpendicular plane (strike 304°, dip 20° to the northeast). The uncertainty of the solution is obtained by a visual comparison between data and synthetics for different focal mechanism solutions.

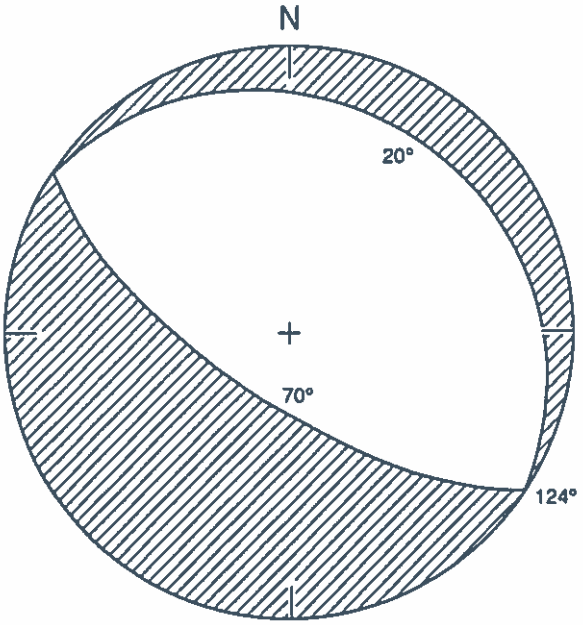

Fig. 7. Fault plane solution of the Roermond earthquake. Equal-area projection of the lower focal hemisphere. Quadrants of compressional P-wave onsets are hatched.

The uncertainty in strike, dip and rake (i.e. angle between the slip direction and the strike) is approximately 10°, where a strike of 114° better models the relative amplitudes than a strike of 134°, and dip of 80° gives a better fit to the data than a dip of 60°. The movement may have had a minor left- or right-lateral component corresponding to a rake of −100° or −80°, instead of −90°. Our optimum focal mechanism solution corresponds remarkably well to the solution obtained by Ahorner (1992) from a large number of first motion readings (strike 124°, dip 68°, rake 90°). Note that this solution was independently obtained using a completely different data set.

The optimum focal mechanism solution is presented in Fig. 7 as a lower hemisphere projection of the nodal planes. This focal mechanism is typical of normal faulting in an extensional stress regime. The northeast extension inferred from the earthquake mechanism points to ongoing subsidence of the Roer Valley Graben. Zijerveld et al. (1992) suggest that present subsidence of the graben is related to the development of the Rhine Graben and controlled by the lithospheric stresses in north-

western Europe. Furthermore, the focal mechanism suggests that faulting may have occurred along the Peel Boundary Fault since the strike and dip direction of the steeply dipping nodal plane are in close agreement with those of that fault. To investigate whether the earthquake is actually located on this fault, we need a more reliable determination of the focal depth. As already mentioned, this requires accurate knowledge of the velocity structure. By modelling the arrival times of the later phases we were able to better constrain both the velocity model and hypocentral depth.

We adjusted the initial velocity structure of Ahorner & Pelzing (1983) to match the arrival times of all phases shown in Fig. 6. Two prominent features were changed (see model P-NL of Fig. 3): a low-velocity sedimentary layer was introduced, and the Moho depth was elevated to 29 km. These features better represent the average velocity structure beneath The Netherlands (see Remmelts & Duin 1990). Note, that the P-wave phases sample the average structure between source and receivers, not only the local structure near the epicenter. The new velocity structure gave a better travel time agreement of nearly all phases. Obviously, our average model is too slow for the nearby stations NE39 and NE33 (see Fig. 5a), which is not surprising due to the known variations in uppermost crustal velocity structure. The importance of the implementation of a low-velocity sedimentary layer for the more distant stations (> 100 km) is shown by the presence of a reflected phase at the base of this layer, denoted as the p(s)P-phase. This phase is very clearly observed at NE31 and NE38, but the other stations also show evidence for its presence.

Using the new velocity model, we found that the arrival times are best matched by a depth of 20 km. An uncertainty of 3 to 4 km remains due to uncertainties in the velocity model and lateral variations in the crustal velocity structure. Thus, the waveform modelling results also point to a deep extension of the seismogenic zone in the region of the Roer Valley Graben.

Lastly, we re-examined the hypothesis of the earthquake occurrence on the Peel Boundary Fault. If we assume that the 70° SW dipping nodal plane represents the fault plane and that the dip does not change with depth, we can calculate the expected location of the fault plane at the surface. For a hypocentral depth of 20 km, the surface expression of the fault will be displaced by 7.2 km (NE) relative to the epicenter, which is in surprisingly good agreement with the location of the Peel Boundary Fault. This substantiates early suggestions that the Roermond earthquake represents a dip-slip movement along this fault. An alternative interpretation of the focal mechanism solution might be that the 20° dipping plane coincides with the fault plane. This would imply low-angle normal faulting along a conjugate, possibly listric, fault. However, the good agreement of the hypocenter and earthquake mechanism with the Peel Boundary Fault makes this interpretation less likely.

Discussion and conclusion

The Roermond earthquake of April 13th, 1992, was investigated using seismograms of the broadband digital NARS network. Although not designed for the recording of such strong local earthquakes, the data of the network tightly constrained the various earthquake parameters. Epicentral location, depth, and the focal mechanism of the event could accurately be determined from the NARS seismograms. We were not able to determine the Richter magnitude of the earthquake due to signal distortion at peak ground motion. The limitations of the current digital recording instruments will be much reduced by the newly designed dataloggers, which will become operational within a year.

This interpretation of the Roermond earthquake by NARS seismograms shows the advantages of good quality data combined with waveform modelling techniques. Synthetic seismograms were used to interpret the signal in terms of the various phases, and to find the optimum agreement with the data in terms of the earthquake mechanism, focal depth and P-velocity structure. A relatively small number of seismograms was sufficient to infer that the Roermond earthquake can be interpreted as a normal faulting event along the Peel Boundary Fault at a remarkably large depth of approximately

20 km. Thus, the earthquake was a deep expression of ongoing subsidence of the Roer Valley Graben in an extensional stress regime. Apart from information about the earthquake itself, the seismograms of the Roermond earthquake also provide information about the relatively unknown deep crustal structure beneath The Netherlands.

Acknowledgements

We like to thank Arie van Wettum, the local NARS station managers, and everybody involved in the NARS data processing for their contribution to the deployment of NARS. Dr. Haak of the seismological department of the Royal Netherlands Meteorological Institute is acknowledged for discussions and information on the Roermond earthquake. NARS is financed by the Earth Science Branch (AWON) of the Netherlands Organization for Scientific Research (NWO).

References

Ahorner, L. 1983 Historical seismicity and present-day microearthquake activity of the Rhenish Massif, Central Europe. In: K. Fuchs et al. (eds). Plateau Uplift. Springer-Verlag, Berlin: 198–221

Ahorner, L. 1992 Das Erdbeben bei Roermond am 13. April 1992, Report Erdbebenstation Bensberg, Abteilung für Erdbebengeologie, Geologisches Institut, Universität Köln, 7 pp

Ahorner, L. & R. Pelzing 1983 Seismotectonische Herdparameter von digital registrierten Erdbeben der Jahre 1981 and 1982 in der westlichen Niederrheinische Bucht – Geol. Jb. (E26): 35–63

Aki, K. & P.G. Richards 1980 Quantitative Seismology: Theory and Methods. W.H. Freeman, San Francisco, 932 pp

Chapman, C.H. 1978 A new method for computing synthetic seismograms – Geophys. J. R. astr. Soc. 54: 481–518

Dost, B. 1987 The NARS array, a seismic experiment in western Europe. Ph.D. thesis (University of Utrecht), 117 pp

Dost, B., A. van Wettum & G. Nolet 1984 The NARS array – Geol. Mijnbouw 63: 381–386

Houtgast, G. 1991 Catalogus van aardbevingen in Nederland. Koninklijk Nederlands Meteorologisch Instituut, de Bilt, 166 pp

Lee, W.H.K. & J.C. Lahr 1972 HYPO71: a computer program for determining hypocenter, magnitude, and first motion pattern of local earthquakes. U.S. Geol. Surv. Open-File Report: 75–311

Lienert, B.R., E. Berg & L.N. Frazer 1986 Hypocenter: an earthquake location method using centered, scaled, and adaptively damped least squares – Bull. Seismol. Soc. Am 76: 771–783

Nolet, G., B. Dost & H. Paulssen 1985 Intermediate wavelength seismology and the NARS experiment – Annales Geophysicae 4: 305–314

Remmelts, G. & E.J.Th. Duin 1990 Results of a regional deep seismic survey in The Netherlands. In: B. Pinet & C. Bois (eds.) The potential of deep seismic profiling for hydrocarbon exploration. Editions Technip, Paris: 335–343

Scholz, C.H. 1990 The mechanics of earthquakes and faulting. Cambridge University Press, Cambridge, 439 pp

Zijerveld, L., R. Stephenson, S. Cloetingh, E. Duin & M.W. van den Berg 1992 Subsidence analysis and modelling of the Roer Valley Graben – Tectonophysics, 208: in press